

Theoretical studies of spin-dependent electronic transport in ferromagnetically contacted graphene flakes

S. Krompiewski

Institute of Molecular Physics, Polish Academy of Sciences, ul. M. Smoluchowskiego 17, 60179 Poznań, Poland

(Received 16 January 2009; revised manuscript received 20 May 2009; published 28 August 2009)

Based on a tight-binding model and a recursive Green's function technique, spin-dependent ballistic transport through tiny graphene sheets (flakes) is studied. The main interest is focused on electrical conductivity, giant magnetoresistance (GMR), and shot noise. It is shown that when graphene flakes are sandwiched between two ferromagnetic electrodes, the resulting GMR coefficient may be quite significant. This statement holds true both for zigzag and armchair chiralities, as well as for different aspect (width/length) ratios. Remarkably, in absolute values the GMR of the armchair-edge graphene flakes is systematically greater than that corresponding to the zigzag-edge graphene flakes. This finding is attributed to the different degree of conduction channel mixing for the two chiralities in question. It is also shown that for big aspect ratio flakes, three-dimensional end-contacted leads, very much like invasive contacts, result in nonuniversal behavior of both conductivity and Fano factor.

DOI: [10.1103/PhysRevB.80.075433](https://doi.org/10.1103/PhysRevB.80.075433)

PACS number(s): 81.05.Uw, 75.47.De, 75.47.Jn

I. INTRODUCTION

Recently a lot of interest has been directed to carbon-based systems, in search for alternative materials which would make it possible to go beyond the silicon technology. While looking at history of studies along this line, one can point out two important milestones: (i) discovery of carbon nanotubes (CNTs), honeycomb-lattice cylinders, dating back to 1991,¹ and (ii) fabrication of individual atomic planes, called graphene (Gr), by exfoliation from graphite in 2004.² So far, on obvious grounds, the CNTs have been much more thoroughly investigated than Gr, but this difference diminishes very quickly. This paper focuses on spin transport problems, mostly on giant magnetoresistance, related to potential applications of graphitic nanostructures in spintronics. In this respect, quite a lot has been done in the case of CNTs: there are hundreds of both experimental³⁻⁷ and theoretical⁸⁻¹¹ papers, covering all the transport regimes (ballistic, Coulomb blockade, Schottky barrier, and Kondo), which show that the giant magnetoresistance (GMR) or tunnel magnetoresistance effects are usually quite considerable. The respective studies on Gr are still scarce. The pioneering experimental paper on magnetoresistance is Ref. 12, where Gr spin valve devices with permalloy contacts have been shown to have the GMR effect $\approx 10\%$ at room temperature. The following experimental paper¹³ reports on conductance of Gr showing Fabry-Pérot-like patterns and pronounced oscillations of GMR (including changes in sign). From the theoretical point of view, the debate is still on, and the question whether or not the Gr-based spin valves have a good performance is still open. The results published so far show that the answer to this question depends critically on the contacts (cf. Ref. 14 and Refs. 15 and 16). In this study, in contrast to those reported hitherto by other theoreticians, three-dimensional contacts are used.

The paper is organized as follows: In Sec. II the theoretical method based on a tight-binding model, as well as the way the graphene sheets and the contacts have been modeled, is shortly outlined. Section III is devoted to presenta-

tion of results, whereas the subsequent section summarizes the main results.

II. METHOD AND MODELING

The method employed here is similar to that used earlier while dealing with carbon nanotubes inserted between ferromagnetic contacts,⁹⁻¹¹ except that carbon allotrope of interest now is graphene. The single π -orbital tight-binding Hamiltonian describes a graphene sheet of width W and length L (in the current direction). The semi-infinite metallic electrodes extend from $\langle -\infty, 0 \rangle$ and $\langle L, \infty \rangle$ for the source and drain, respectively. The ferromagnetic electrodes are supposed to have spin-split s bands, mimicking d bands of real transition metals. The total Hamiltonian reads

$$H = - \sum_{i,j,\sigma} t_{i,j} |i,\sigma\rangle \langle \sigma,j| + \sum_{i,\sigma} \epsilon_{i,\sigma} |i,\sigma\rangle \langle \sigma,i|, \quad (1)$$

where i and j run over the whole device (i.e., graphene and the electrodes), σ is the spin index, and $t_{i,j}$ and $\epsilon_{i,\sigma}$ stand for the hopping integrals and the on-site potentials, respectively. The systems under study are impurity free with well transparent interfaces (strong-coupling limit) so neglecting of correlations in the Hamiltonian should be justified if one restricts oneself just to the ballistic transport regime, putting aside the Coulomb blockade^{6,17} and Kondo^{5,7} regimes. In this regard, the on-site parameters in the present approach are used to take into account the effect of the gate voltage in the graphene sheet as well as the spin band splitting in the metallic electrodes.

Figure 1 shows schematically devices of the present interest, viz., zigzag-edge graphene (zz-Gr) and armchair-edge graphene (ac-Gr). The graphene sheets (black spheres) are sandwiched between metallic contacts (light spheres). The diameters of the spheres correspond to the nearest-neighbor spacings. The unit cells in the vertical direction are the blunt saw-teeth lines for zz-Gr, and double zigzag lines for ac-Gr. As readily seen, it is assumed that there is a perfect lattice

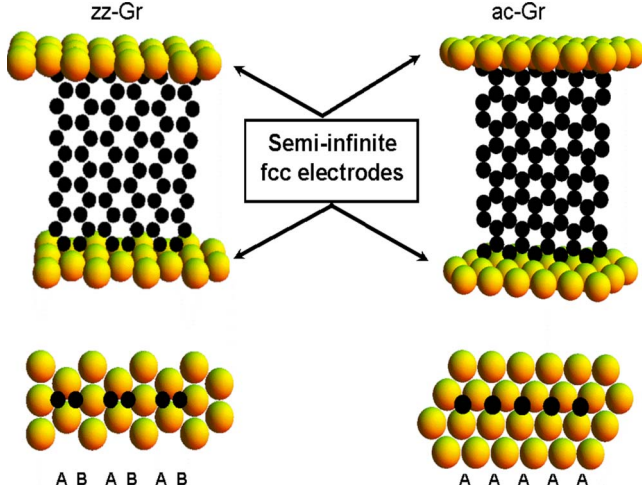


FIG. 1. (Color online) Graphene sheets attached to semi-infinite three-dimensional metallic electrodes. The left and right parts correspond to the zigzag- and armchair-edge ribbons, respectively. The lower part shows details of the interfaces, whereas the letters *A* and *B* denote a type of the sublattice the interface carbon atoms belong to.

matching between graphene and the electrodes. In fact this assumption is acceptable since the graphene lattice constant ($a_{Gr}=2.46 \text{ \AA}$) fits really well to interatomic distances in such metals like Cu(2.51 \AA), Ni(2.49 \AA), or Co(2.55 \AA).¹⁸

The use of single-orbital electrodes allows writing an analytic expression for the electrodes surface Green's functions in \mathbf{k} space,

$$g_{\sigma}(\mathbf{k}, E) = \frac{E - \epsilon_{\sigma}(\mathbf{k}) \pm \sqrt{[E - \epsilon_{\sigma}(\mathbf{k})]^2 - 4|w(\mathbf{k})|^2}}{2|w(\mathbf{k})|^2},$$

$$\epsilon_{\sigma}(\mathbf{k}) = 2t \left(\cos k_x a + 2 \cos \frac{k_x a}{2} \cos \frac{\sqrt{3} k_y a}{2} \right) + \Delta_{\sigma},$$

$$w(\mathbf{k}) = -t \left[2 \cos \left(\frac{k_x a}{2} \right) e^{ik_y a / 2\sqrt{3}} + e^{-ik_y a / \sqrt{3}} \right], \quad (2)$$

where $a = \sqrt{2}a_{Gr}$ is the fcc-metal lattice constant, g_{σ} is the surface Green function for spin σ , and Δ_{σ} is a rigid-band splitting chosen so as to give a desirable spin polarization P of the electrodes. Here $P=50\%$ has been set, corresponding to $\Delta_{\uparrow} = -2.32t$ and $\Delta_{\downarrow} = 1.6t$ (in the paramagnetic case $\Delta_{\sigma} = -0.86t$). Incidentally, this simple parametrization has already been shown to work satisfactorily well in the case of carbon nanotube/ferromagnet systems.^{9,10} $\epsilon_{\sigma}(\mathbf{k})$ in Eq. (2) is the fcc(111)-surface energy spectrum, calculated for a semi-infinite metal slab according to the method described in Ref. 19. The surface k vectors lie on the metal surface, but upon attachment of graphene they are no longer good quantum numbers, so the trick is to perform a Fourier transformation to the real space and work with those surface Green's functions which are close to the graphene interface. After having transformed the surface Green's function to the real space, the self-energies Σ_{σ}^{α} and the corresponding spectral functions Γ_{σ}^{α} are computed from $\Sigma_{\sigma}^{\alpha} = T g_{\sigma}^{\alpha} T^{\dagger}$ and $\Gamma_{\sigma}^{\alpha} = i(\Sigma_{\sigma}^{\alpha} - \Sigma_{\sigma}^{\alpha\dagger})$, re-

spectively. With $\alpha=L$ or R , referring the left and right electrodes, and T being the Gr/electrode coupling matrices. Henceforth, the spin indexes σ will be skipped for brevity.

The recursive method goes as follows:²⁰

$$g_L(0) \equiv g_L, g_R(N+1) \equiv g_R,$$

$$g_{L,R}(i) = [E - D_i - \Sigma_{L,R}(i)]^{-1},$$

$$\Sigma_L(i) = T_{i,i-1} g_L(i-1) T_{i-1,i},$$

$$\Sigma_R(i) = T_{i,i+1} g_R(i+1) T_{i+1,i}, \quad (3)$$

$$G_i = [E - D_i - \Sigma_L(i) - \Sigma_R(i)]^{-1}. \quad (4)$$

Above, $g_{L,R}$ are local Green's functions for the i th unit cell of graphene, the matrices D and T stand for the diagonal and off-diagonal Hamiltonian submatrices, whereas the full Green's function is given by Eq. (4). The graphene unit cells extend from $i=1$ (following the L electrode) up to $i=N$ (preceding the R electrode). So the recursion starts with the metal-interface Green's functions $g_L(0)$ and $g_R(N+1)$ being Fourier components of the surface Green's functions defined in Eq. (2).

The other quantities of interest are transmission (\mathcal{T}), conductivity (σ), and shot-noise Fano factor (F), as well as GMR. In the ballistic transport regime and at zero temperature, these quantities read

$$\mathcal{T} = \Gamma_i^L G_i \Gamma_i^R G_i^{\dagger},$$

$$\sigma = (L/W) \frac{e^2}{h} \text{Tr}[\mathcal{T}(E_F)],$$

$$F = \text{Tr}\{\mathcal{T}(E)[1 - \mathcal{T}(E)]\} / \text{Tr}[\mathcal{T}(E)],$$

$$\text{GMR} = 100(1 - \sigma_{\uparrow,\downarrow} / \sigma_{\uparrow,\uparrow}), \quad (5)$$

where the arrows $\uparrow\uparrow$ and $\uparrow\downarrow$ denote parallel and antiparallel alignments of ferromagnetic electrodes.

III. RESULTS

We use Eqs. (5) to determine the quantities of our main interest. At first, for comparison, we have calculated GMR for zz-Gr and ac-Gr sheets vs energy which, in principle, is proportional to the gate voltage. From the results in Fig. 2 one can see that GMR, at least in the ac-Gr case, is quasiperiodic with the period length roughly proportional to the aspect ratio A , i.e., inverse proportional to the length of the graphene sheets L . Numerically, the periods are close to the well-established value $p \cong 2 \text{ eV}/L[\text{nm}]$,²¹ or in the present units $p \cong 0.8 \text{ A}/W[\text{nm}]$ (the energy unit is $t=2.7 \text{ eV}$). Incidentally, some features characteristic for Fabry-Pérot resonances in graphene have been already reported,^{21,22} where it has been also stressed that irregularities and defects of graphene edges may turn the conventional Fabry-Pérot picture into a spectacular quantum billiard-type one. It is seen in Fig. 2 that the GMR factors for ac-Gr and zz-Gr differ in

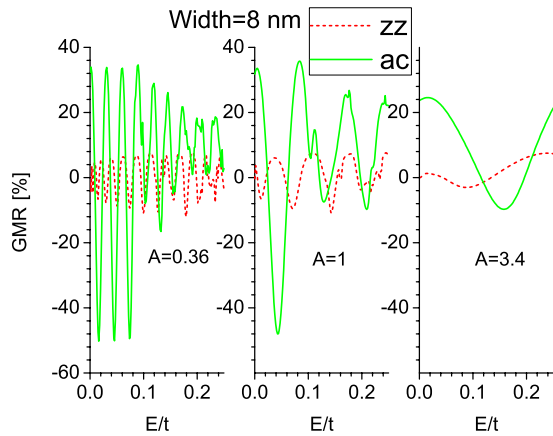


FIG. 2. (Color online) Giant magnetoresistance for ac-Gr (solid curve) and zz-Gr (dash curve) flakes vs energy, and for three different aspect ratios. Note that the number of quasiperiods is roughly inverse proportional to A (i.e., proportional to the length), meaning that Fabry-Pérot-like resonances take place.

three respects: (i) magnitude, (ii) the maxima of the former are roughly equidistant in contrast to the latter, moreover (iii) in the former the onset of the second subband is visible (at $E \cong 0.08$, except for $A=3.4$, where $W > L$), whereas in the latter it always is washed out. Qualitatively these results, showing that GMR vs energy (gate voltage) changes also in sign, are consistent with the experiment of Ref. 13.

Another interesting point encountered here, is the universal behavior issue due to evanescent modes at the Dirac points. It is well known that graphene sheets of large sizes, with $W \rightarrow \infty$ and $L \rightarrow \infty$ (with $W > L$), if homogenous, reveal universal values of $\sigma = 4/\pi e^2/h$ and $F = 1/3$.^{21,23,24} The term “homogenous” in this context means that the device at hand is an all-carbon system, typically, with a central graphene sheet, and highly doped graphene electrodes. This theoretical concept might be quite realistic for widely applied experimental setups with *side-contacted* graphene sheets, provided evaporated metal contacts are not invasive, i.e., they do not destroy the underlying honeycomb lattice but merely dope it slightly. It has been also shown theoretically that in the case of *end-contacted* devices to two-dimensional square-lattice contacts, the situation is more complicated and respective values of the conductivity and the Fano factor do depend on the on-site potentials in electrodes and on details of bonds between square-lattice electrodes and graphene.²⁵ Importance of the interface conditions which determine, *inter alia*, mixing of propagating modes, and whether or not the momentum component along the interface direction is conserved, has been noticed in Refs. 25–31. It has been also demonstrated using one-parameter scaling arguments that at the Dirac points, conductivity of an infinitely large graphene with disorder is infinite (zero) if there is no (there is) intervalley scattering.³² Beyond the Dirac points the evanescent modes give way to the propagating ones, and in the ballistic transport regime, perfect noiseless transmission due to Fabry-Pérot resonances may take place.^{13,33}

Figure 3 clearly shows that this scenario also holds in the ferromagnetic case for ac-Gr if the aspect ratio is not too big (Gr ribbon is long enough). Indeed maxima in σ (inset cor-

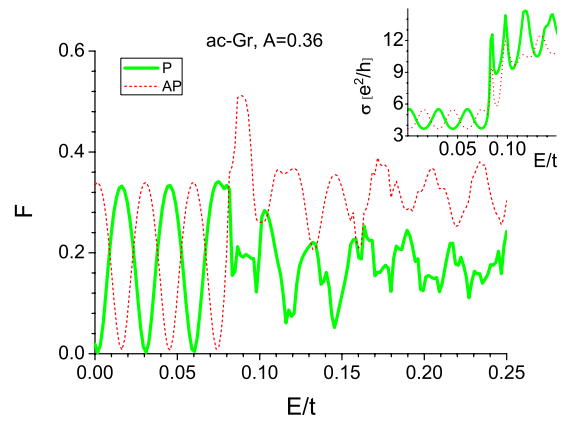


FIG. 3. (Color online) Shot noise Fano factor for the armchair graphene ~ 8 nm in width and with the aspect ratio $A=0.36$: for ferromagnetic electrodes (parallel alignment—thin solid line; and antiparallel alignment—dash line). Inset presents the respective conductivities.

respond to minima of F (at $F=0$) in the main panel. In the zz-Gr case with the same A value, the situation is similar (not plotted), but then the oscillations in the P and AP configurations are not phase shifted.

As regard to Gr sheets with bigger A , Figs. 4 and 5 show some features of F and σ , which happen to be similar to the universal ones when the Gr sheets are paramagnetically contacted (thick black lines). However, if the contacts are ferromagnetic there is a tendency for F to increase and for σ to decrease. This suggests that in general Gr flakes studied here show nonuniversal behavior, which is to be attributed to the finite sizes, and the inhomogeneity resulting in contact-dependent charge transfer between interface atoms (and accompanying electron-hole asymmetry). Incidentally, the present approach was shown earlier to yield short-range charge transfer, affecting mainly interface carbon monolayers.^{10,20} As a matter of fact, the nonuniversal behavior of F and σ in Gr systems has been already reported to be due to: charged impurity scattering,³⁴ strong disorder,³⁵ and invasive contacts.^{36,37}

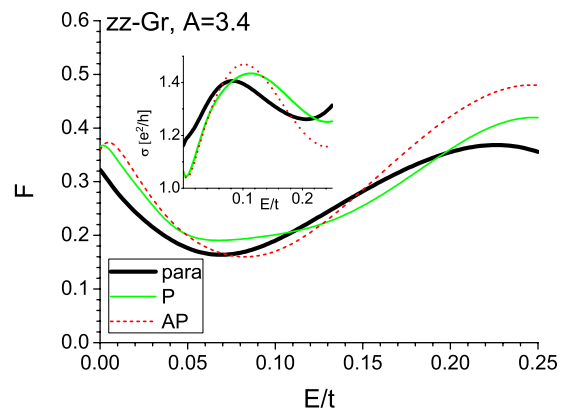


FIG. 4. (Color online) Shot noise Fano factor for the zigzag graphene ~ 8 nm in width and with the aspect ratio $A=3.4$: for paramagnetic electrodes (thick solid line), ferromagnetic electrodes (parallel alignment—thin solid line; antiparallel alignment—dash line). Inset presents the respective conductivities.

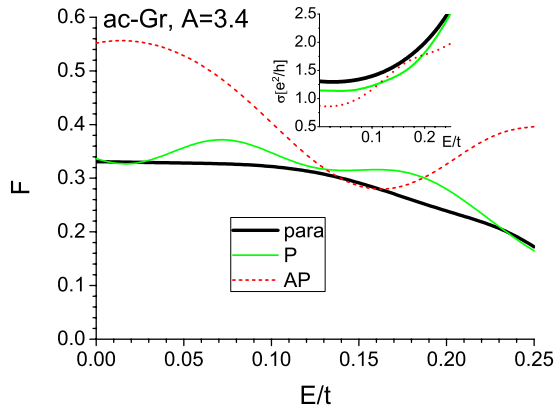


FIG. 5. (Color online) Same as Fig. 4 but for armchair-edge graphene.

Finally, it should be noted that the results presented in Figs. 2–5 hardly depend on the hopping parameters as long as the interfaces are transparent enough. In the present theory this condition is fulfilled provided the hopping parameter across the interface (t_c) is not too different from the geometric mean of hopping parameters for the metal electrodes (t_M) and graphene (t), i.e., from $t_c = \sqrt{t_M t}$. Otherwise, in case of a drastic differentiation of the hopping parameters, and opaque interfaces (very small t_c) the Coulomb blockade physics may come into play,¹⁷ out of reach of the present approach.

IV. CONCLUSION

Summarizing, the aim of this study has been to estimate the effect of the chirality as well as the aspect ratio on the GMR coefficient of graphene flakes end-contacted to ferromagnetic electrodes. In contrast to other theoretical approaches, the leads are not supposed here to be two-dimensional (of honeycomb- or square-lattice type), but

more realistically they are modeled as three-dimensional fcc-(111) semi-infinite slabs. It turns out that for long and narrow systems (small aspect ratio), the GMR is a quasiperiodic function of energy (gate voltage) with the period roughly proportional to the aspect ratio, reflecting Fabry-Pérot-like resonances, typical of ballistic transport. Notably, the GMR coefficient of the ac-Gr flakes may exceed 20%–40%, depending on the aspect ratio value, whereas for zz-Gr flakes the corresponding figures are distinctly smaller, but still significant. The difference is due to the fact that in the case of armchair-edge sheets, all the interface carbon atoms belong to the same sublattice (say, A type), as opposed to the zigzag ones with interface carbon atoms of both A and B type. This inevitably facilitates intervalley mode mixing in the latter case. Another noteworthy point, in the context of zero-energy (Dirac-point) conductivity and Fano factor, is that for the big aspect ratio. Such systems studied here show nonuniversal behavior when ferromagnetic electrodes are applied. It is so even if the corresponding values for the paramagnetic electrodes happen to be close to the universal ones ($4/\pi e^2/h$ and $1/3$ for σ and F , respectively). However, these systems are inhomogeneous and rather small, so neither the limits $W \rightarrow \infty$ and $L \rightarrow \infty$ (with $W > L$) nor the requirement of a large number of propagating modes can be fulfilled (see the relevant assumptions in Ref. 23). It is noteworthy that the wide end-contacted devices considered here resemble experimental setups with invasive contacts, which do not show universal behavior either.

ACKNOWLEDGMENTS

This work was supported by the EU FP6 grant CARDEQ under Contract No. IST-021285-2 and, as part of the European Science Foundation EUROCORES Programme SPIN-TRA (Contract No. ERAS-CT-2003-980409), by the Ministry of Science and Higher Education as a research project in 2006-2009.

¹S. Iijima, *Nature (London)* **354**, 56 (1991).

²K. S. Novoselov, A. K. Geim, S. V. Morozov, D. Jiang, Y. Zhang, S. V. Dubonos, I. V. Grigorieva, and A. A. Firsov, *Science* **306**, 666 (2004).

³K. Tsukagoshi, B. W. Alphenaar, and H. Ago, *Nature (London)* **401**, 572 (1999).

⁴S. Sahoo, T. Kontos, J. Furer, C. Hoffmann, M. Graber, A. Cottet, and C. Schönberger, *Nat. Phys.* **1**, 99 (2005).

⁵J. R. Hauptmann, J. Paaske, and P. E. Lindelof, *Nat. Phys.* **4**, 373 (2008).

⁶W. Liang, M. Bockrath, and H. Park, *Phys. Rev. Lett.* **88**, 126801 (2002).

⁷S. Sapmaz, P. Jarillo-Herrero, J. Kong, C. Dekker, L. P. Kouwenhoven, and H. S. J. van der Zant, *Phys. Rev. B* **71**, 153402 (2005).

⁸H. Mehrez, J. Taylor, H. Guo, J. Wang, and C. Roland, *Phys. Rev. Lett.* **84**, 2682 (2000).

⁹S. Krompiewski, *Phys. Status Solidi B* **242**, 226 (2005).

¹⁰S. Krompiewski, *Semicond. Sci. Technol.* **21**, S96 (2006).

¹¹S. Krompiewski, *Nanotechnology* **18**, 485708 (2007).

¹²E. Hill, A. K. Geim, K. Novoselov, F. Schedin, and P. Blake, *IEEE Trans. Magn.* **42**, 2694 (2006).

¹³S. Cho, Yung-Fu Chen, and M. S. Fuhrer, *Appl. Phys. Lett.* **91**, 123105 (2007).

¹⁴L. Brey and H. A. Fertig, *Phys. Rev. B* **76**, 205435 (2007).

¹⁵Woo Youn Kim and Kwang S. Kim, *Nat. Nanotechnol.* **408**, 3 (2008).

¹⁶K. H. Ding, Z. G. Zhu, and J. Berakdar, *Phys. Rev. B* **79**, 045405 (2009).

¹⁷I. Weymann, J. Barnaś, and S. Krompiewski, *Phys. Rev. B* **78**, 035422 (2008).

¹⁸V. M. Karpan, G. Giovannetti, P. A. Khomyakov, M. Talanana, A. A. Starikov, M. Zwierzycki, J. van den Brink, G. Brocks, and P. J. Kelly, *Phys. Rev. Lett.* **99**, 176602 (2007).

¹⁹T. N. Todorov, G. A. D. Briggs, and A. P. Sutton, *J. Phys.: Condens. Matter* **5**, 2389 (1993).

- ²⁰S. Krompiewski, *J. Phys.: Condens. Matter* **16**, 2981 (2004).
- ²¹F. Miao, S. Wijeratne, Y. Zhang, U. C. Coskun, W. Bao, and C. N. Lau, *Science* **317**, 1530 (2007).
- ²²L. A. Ponomarenko, F. Schedin, M. I. Katsnelson, R. Yang, E. W. Hill, K. S. Novoselov, and A. K. Geim, *Science* **320**, 356 (2008).
- ²³J. Tworzydło, B. Trauzettel, M. Titov, A. Rycerz, and C. W. J. Beenakker, *Phys. Rev. Lett.* **96**, 246802 (2006).
- ²⁴R. Danneau, F. Wu, M. F. Craciun, S. Russo, M. Y. Tomi, J. Salmilehto, A. F. Morpurgo, and P. J. Hakonen, *Phys. Rev. Lett.* **100**, 196802 (2008).
- ²⁵R. L. Dragomirova, D. A. Redskin, and B. K. Nikolić, *Phys. Rev. B* **79**, 241401(R) (2009).
- ²⁶Ya. M. Blanter and I. Martin, *Phys. Rev. B* **76**, 155433 (2007).
- ²⁷J. P. Robinson and H. Schomerus, *Phys. Rev. B* **76**, 115430 (2007).
- ²⁸Eduardo J. H. Lee, Kannan Balasubramanian, Ralf Thomas Weitz, Marko Burghard, and Klaus Kern, *Nat. Nanotechnol.* **3**, 486 (2008).
- ²⁹R. Golizadeh-Mojarad and S. Datta, *Phys. Rev. B* **79**, 085410 (2009).
- ³⁰S. Russo, M. F. Craciun, M. Yamamoto, A. F. Morpurgo, and S. Tarucha, arXiv:0901.0485 (unpublished).
- ³¹P. Blake, R. Yang, S. V. Morozov, F. Schedin, L. A. Ponomarenko, A. A. Zhukov, R. R. Nair, I. V. Grigorieva, K. S. Novoselov, and A. K. Geim, *Solid State Commun.* **149**, 1068 (2009).
- ³²J. H. Bardarson, J. Tworzydło, P. W. Brouwer, and C. W. J. Beenakker, *Phys. Rev. Lett.* **99**, 106801 (2007).
- ³³J. Cayssol, B. Huard, and D. Goldhaber-Gordon, *Phys. Rev. B* **79**, 075428 (2009).
- ³⁴J.-H. Chen, C. Jang, S. Adam, M. S. Fuhrer, E. D. Williams, and M. Ishigami, *Nat. Phys.* **4**, 377 (2008).
- ³⁵C. H. Lewenkopf, E. R. Mucciolo, and A. H. Castro Neto, *Phys. Rev. B* **77**, 081410(R) (2008).
- ³⁶B. Huard, N. Stander, J. A. Sulpizio, and D. Goldhaber-Gordon, *Phys. Rev. B* **78**, 121402(R) (2008).
- ³⁷Xu Du, Ivan Skachko, and Eva Y. Andrei, *Int. J. Mod. Phys. B* **22**, 4579 (2008).